doi:10.1017/S1431927620021352
Microsc. Microanal. 26 (Suppl 2), 2020

Strain Patterning *via* Spontaneous Centroidal Voronoi Tessellation in Few-Layer MoS_2

Yichao Zhang and David Flannigan

University of Minnesota, Minneapolis, Minnesota, United States

Owing to the anisotropic bonding motif inherent to transition metal dichalcogenides (TMDs), these materials can withstand significant elastic strains on the order of 10% and display an associated wide range of variable optical and electronic properties [1]. In addition to interest in fundamental behaviors, such properties have driven efforts to develop strain-tunable devices and applications. While spontaneous wrinkle formation in few to monolayer specimens generates local strain variations, controllable and predictable strain-pattern formation requires rational engineering design and processing principles [2,3]. Nascent approaches have focused on either whole-flake deformation or single, site-specific mechanical indentation to modulate the global or local elastic strain through repeatable stress application. For example, elastomeric films supporting few to monolayer flakes have been used to apply reversible, whole-flake uniaxial strains, while local, nanoscale indentation with AFM tips has been used to quantify elastic stress-strain properties as a function of layer number [4,5]. Spatially periodic strain patterning has been introduced as a way to produce predictable and highly-symmetric local structural modulations in a passive, non-continuous manner (*i.e.*, without the need for constant applied stress). This has been done, for example, by using periodic arrays of nanoparticles blanketing a substrate, followed by flake deposition [6,7]. In this way, local strain can be patterned and controlled by manipulating nanoparticle geometry and patterning periodicity.

Here we report a method for highly-symmetric, spontaneous strain patterning of few-layer MoS_2 using patterned holey substrates and based on the principle of tessellation. In this approach, the centers of the holes in the substrate serve as the generating points for the tessellation patterns. Because the holes are of equivalent diameter and are arranged in a uniformly-spaced, hexagonally-symmetric pattern throughout the substrate, the resulting tessellation pattern in the few-layer MoS_2 flakes displays six-fold rotational symmetry that is well-described by centroidal Voronoi tessellation (Figure 1a). In a bright-field image, the tessellation manifests as strongly-scattering bend contours running between the substrate holes and forming three-fold vertices at the center of sets of three holes. Further, twelve-fold bend contours, which can be indexed to first- and second-order Bragg spots, form in the center of the tessellated hexagons and the substrate holes, as confirmed with correlated bright- and dark-field imaging (Figure 1b). The bend contours radiate from the center of the generating points and arise from uniform strain-induced curvature of the few-layer flake over the substrate hole. In addition to spontaneous formation, tessellated strain-patterning is also influenced by the deposition of polymer residue on top of the flake within the holes during exfoliation and flake mounting on the substrate (Figure 1c). Spatially-averaged strains of 1% to 3% in the MoS_2 flake are present over the holes, as determined with selected-area diffraction. Further, spatial mapping of relative strain in correlation with the image contrast was performed with nanobeam electron diffraction (NBED) with a 10-nm incident beam size (Figure 1d). In this way, maximum strains were found to be present near the center of the holes at the tessellation generating points, with a steep strain gradient to lower values moving toward the substrate before again increasing while approaching the hexagonal tessellation patterns over the substrate (Figure 1e). These results suggest a simple, highly-repeatable method based on principles of tessellation for producing highly-symmetric, strain-patterned films of high regular periodicity in TMDs, other layered materials, and generally in ultrathin films and crystals [8].

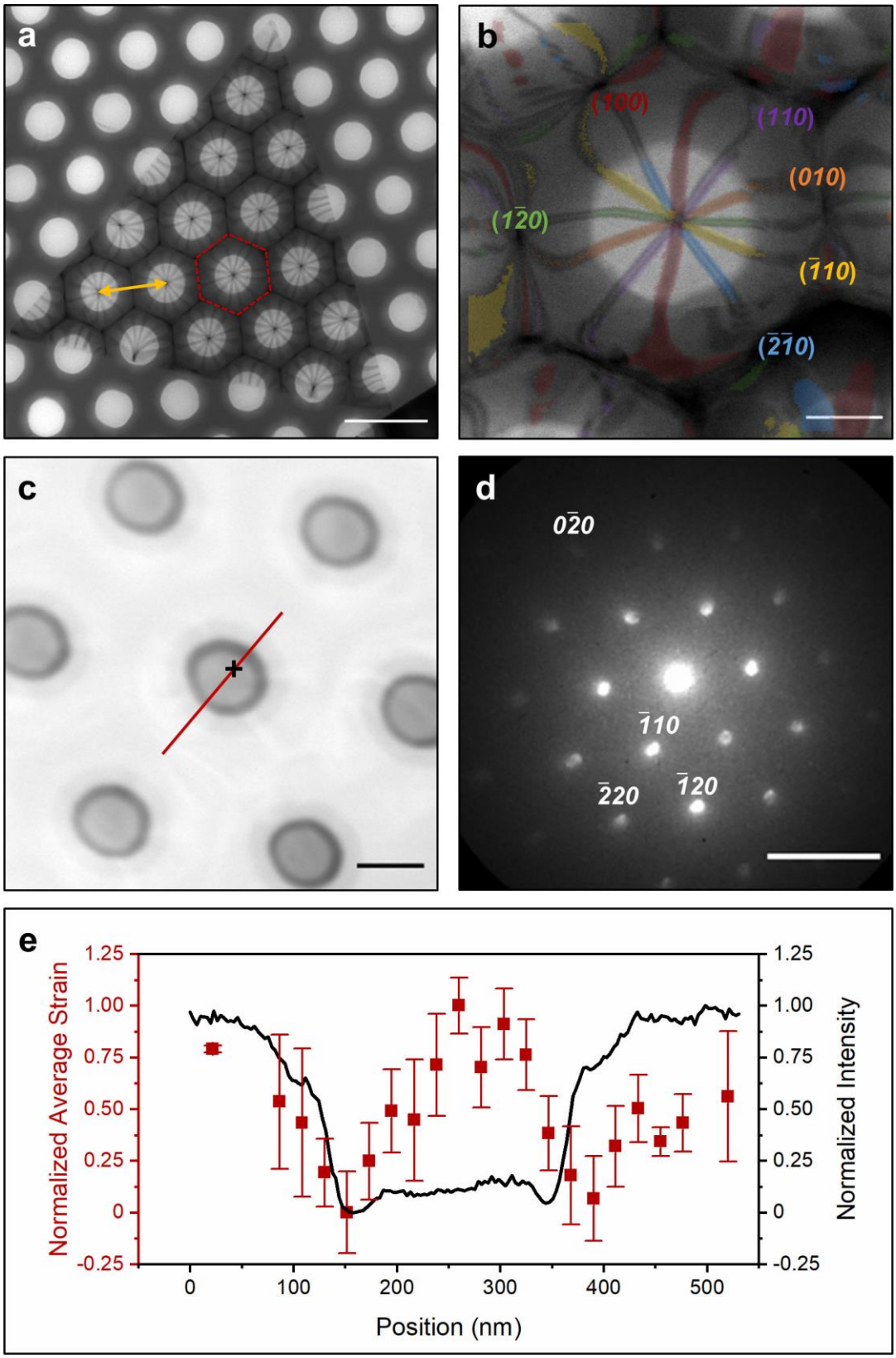

Figure 1. Spontaneous strain patterning in few-layer MoS2 via centroidal Voronoi tessellation. (a) Low-magnification bright-field TEM image of a few-layer MoS2 flake displaying hexagonal centroidal

https://doi.org/10.1017/S1431927620021352 Published online by Cambridge University Press

Voronoi tessellation. The dashed red hexagon highlights one unit cell of the tessellation pattern (edge length = 236 nm). The yellow double-headed arrow marks the distance between two tessellation generating points centered over substrate holes. The scale bar represents 500 nm. (b) Correlated bright- and dark-field imaging of the twelve-fold bend contours (indexed and false colored) arising from first- and second-order Bragg reflections. The scale bar represents 100 nm. (c) HAADF image of the few-layer MoS2 with polymer residue in the substrate holes. The red line marks the position along which a series of NBED patterns were collected. The scale bar represents 200 nm. (d) Sample NBED pattern obtained at the position marked with the black "+" in panel (c). The indexed Bragg spots were generally used to determine the relative strain in the MoS2 flake. The scale bar represents 5 nm-1. (e) Correlation between the normalized average strain profile determined with NBED and the normalized HAADF image intensity along the red line in panel (c). Error bars represent one standard deviation from the average relative strain determined from the indexed Bragg spots in panel (d).

References

[1] H.-Y. Chang, *et al*., ACS Nano **7** (2013), p. 5446.
[2] P. Miró, M. Ghorbani-Asl, and T Heine, Adv. Mater. **25** (2013), p. 5473.
[3] J. Brivio, D. T. L. Alaxander, and A. Kis, Nano Lett. **11** (2011), p. 5148.
[4] S. Bertolazzi, J. Brivio, and A. Kis, ACS Nano **5** (2011), p. 9703.
[5] A. Castellanos-Gomez, *et al*., Nano Lett. **13** (2013), p. 5361.
[6] H. Li, *et al*., Nat. Commun. **6** (2015), 7381.
[7] Y. Zhang, *et al*., Nano Lett. **18** (2018), p. 2098.
[8] This material is based upon work supported by the National Science Foundation under Grant No. DMR-1654318. This work was supported partially by the National Science Foundation through the University of Minnesota MRSEC under Award Number DMR-1420013.